Chemical Science

EDGE ARTICLE

View Article Online
View Journal | View Issue

Cite this: *Chem. Sci.*, 2015, **6**, 7222

Semiconductive 3-D haloplumbate framework hybrids with high color rendering index white-light emission†

Guan-E Wang, Gang Xu,* Ming-Sheng Wang, Li-Zhen Cai, Wen-Hua Li and Guo-Cong Guo*

Received 11th July 2015
Accepted 17th September 2015

DOI: 10.1039/c5sc02501j

www.rsc.org/chemicalscience

Single-component white light materials may create great opportunities for novel conventional lighting applications and display systems; however, their reported color rendering index (CRI) values, one of the key parameters for lighting, are less than 90, which does not satisfy the demand of color-critical upmarket applications, such as photography, cinematography, and art galleries. In this work, two semiconductive chloroplumbate (chloride anion of lead(II)) hybrids, obtained using a new inorganic–organic hybrid strategy, show unprecedented 3-D inorganic framework structures and white-light-emitting properties with high CRI values around 90, one of which shows the highest value to date.

Introduction

Multi-functional materials possessing both luminescence and semiconductive properties have played a critical role in solid-state lighting (SSL) techniques.[1] Materials with good electrical properties are able to convert electricity to light in a much higher efficiency and smaller devices than conventional incandescent or fluorescent lighting sources. Realizing white-light luminescence is the key step for SSL to become alternative conventional lighting and display systems. The most used method to produce white-light luminescence is a multi-component strategy. This strategy includes three parts: one is to excite a yellow phosphor (or multi-phosphors) using a blue (or UV) light-emitting diode (LED); another one is to blend red, green and blue LEDs;[2] a third is to excite a white phosphor using a UV light source.[3] Multi-component strategies can provide good color-rendering properties, but suffer from efficiency loss owing to self-absorption as well as emission color changes due to individual phosphors degrading at different rates.[4] A single-component strategy is an alternative strategy to generate white-light luminescence.[5] It can overcome the drawbacks of multi-component strategies and has advantages such as improved stability, easier fabrication process, and better color reproducibility.[6] However, it is still a big challenge to obtain a single-component material with high quality white-light luminescence.

The color rendering index (CRI) is a very important parameter of SSL devices and full-color display systems.[7] It describes how well a light source renders the colors of an object compared to an incandescent light or daylight. The CRI has a scale from 0 to 100 percent and the higher its value, the better its color rendering ability. A source with a CRI of 70 is acceptable for normal lighting applications, while a CRI of 80 is needed for human eye-friendly applications. An ultra-high CRI (above 90) is required to satisfy the demands of color-critical high-level applications, such as photography, cinematography, art galleries, jewellery, surgery, and cosmetic sales counters. With very high cost, an ultra-high CRI multi-component system can be obtained by carefully balancing the emitting intensities of different colors.[8] However, an ultra-high CRI of a single-component system has not been reported yet. As far as we know, most reported single-component materials have CRI values less than 85.[9] The photoluminescence spectrum of a single-component white-light emitting phosphor normally shows a very broad peak with a fixed ratio of different colors. Therefore, to individually tune the emitting intensities of different colors is very difficult in this case.

Crystalline inorganic–organic hybrids have shown great achievements in single-component white-light emitting phosphors,[5a] but an ultra-high CRI has not been realized. In a hybrid system, white light mainly comes from broad emission of the inorganic components.[9a,b] One possible way to improve the CRI is to involve an organic emitting center in a hybrid. A hybrid material system normally has a weak interaction between the inorganic and organic components which makes it possible to design a hybrid with very weak electronic communication between the inorganic and organic components. Therefore, when the inorganic and organic components are selected to separately have blue and yellow/orange emitting centers, and a

State Key Laboratory of Structural Chemistry, Fujian Institute of Research on the Structure of Matter, Chinese Academy of Sciences, Fuzhou, Fujian 350002, P. R. China. E-mail: gxu@fjirsm.ac.cn; gcguo@fjirsm.ac.cn

† Electronic supplementary information (ESI) available. CCDC 1055380 and 1055381. For ESI and crystallographic data in CIF or other electronic format see DOI: 10.1039/c5sc02501j

partially overlapped excitation band, the result would be that: (1) the overlapped excitation band can activate blue and yellow/orange emission synchronously; (2) multi-emitting centers are independently tunable to balance the ratio of the emissions of different colors by shifting the exciting wavelength. In this manner, white-light emission of this hybrid material can be realized and its CRI can be tuned to a high value. Moreover, the inorganic component can be selected to provide good electrical properties for the hybrid material.[10] Thus, a multifunctional hybrid with both good conductivity and interesting light emission might be designed and created.

Here, we report a single-component white-light emitting compound with a CRI as high as 96, which is the highest value to date. Using an inorganic–organic hybrid strategy, two crystalline hybrids, $(H_2DABCO)(Pb_2Cl_6)$ (**1**) and $(H_3O)(Et_2\text{-}DABCO)_8(Pb_{21}Cl_{59})$ (**2**), (DABCO = 1,4-diazabicyclo[2.2.2]-octane; Et = ethyl) were synthesized. Single crystal X-ray diffraction measurements revealed their unique lead halide based three-dimensional (3-D) inorganic framework structures. These two hybrids have independently tunable organic blue emitting components and inorganic yellow/orange emitting components for high CRI white-light emission. Photoluminescence (PL) studies showed that compound **1** has a cold-white-light emission with a CRI of 96 and compound **2** has a warm-white-light emission with a CRI of 88. In addition, electrical studies of **1** and **2** revealed their typical semiconductive properties.

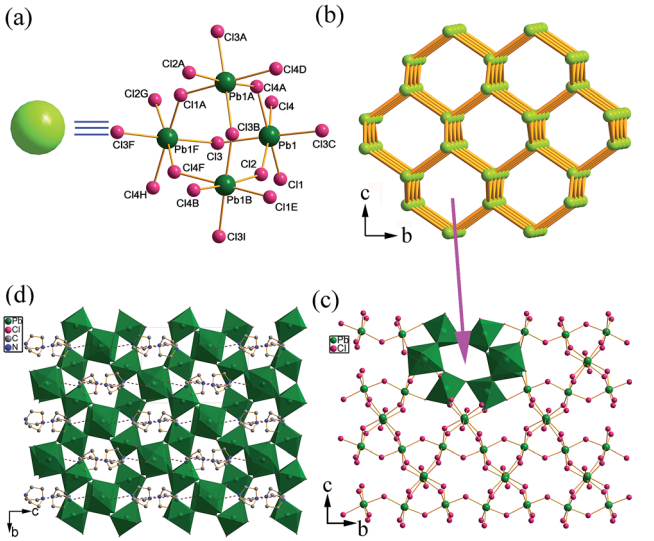

Fig. 1 For **1**: (a) topological node of the Pb_4Cl_{18} cluster; (b) topological diamond structure of the $(Pb_2Cl_6)^{2-}$ ions; (c) structure of the $(Pb_2Cl_6)^{2-}$ framework viewed along the *a* axis, where parts of the Pb octahedra are shown as polyhedra; (d) crystal structure of compound **1** viewed along the *a* direction. Hydrogen atoms are omitted for clarity. The organic $(H_2DABCO)^{2+}$ cations were accommodated in the hexagonal channels through N–H···Cl (with a mean N1···Cl3 separation of 3.263(11) Å, and a mean N1–H···Cl3 angle of 139.1(7)°) hydrogen bonding interactions. Symmetric code: (A) 1.5 − *y*, 0.5 + *x*, −0.25 + *z*; (B) −1 + *y*, 1 + *x*, −1 − *z*; (C) 0.5 + *x*, 2.5 − *y*, −0.75 − *z*; (D) 1 − *x*, 2 − *y*, −0.5 + *z*; (E) 1 − *x*, 3 − *y*, −0.5 + *z*; (F) −0.5 + *x*, 2.5 + *y*, −0.75 − *z*; (G) −1.5 + *y*, 1.5 − *x*, 0.25 + *z*; (H) 1 − *y*, 2 − *x*, −0.5 − *z*; (I) 1.5 − *y*, 1.5 + *x*, −0.25 + *z*.

Results and discussion

Colorless crystals of **1** and **2** were obtained by the solvothermal treatment of $PbCl_2$ and DABCO in ethanol and *n*-butanol, respectively. Detail of the synthesis is shown in the ESI.† Their phase purity was verified by elemental analysis and powder X-ray diffraction (PXRD) determination (see the Experimental section and Fig. S1 in the ESI†).

Single-crystal X-ray diffraction analysis reveals that compound **1** crystallizes in the tetragonal space group $P4_32_12$. The structure of **1** is composed of a unique 3-D $(Pb_2Cl_6)^{2-}$ framework hosting organic $(H_2DABCO)^{2+}$ cations (Fig. 1d). Notably, metal halide-based hybrids normally have 0-D, 1-D or 2-D inorganic structures; 3-D inorganic framework structures have rarely been obtained previously.[11] As shown in Fig. S2,† there is one crystallographically independent Pb atom and four Cl atoms, and each Pb atom is situated in a slightly distorted octahedral coordination environment. From the topological point of view, the four corners shared by $PbCl_6$ octahedra form a Pb_4Cl_{18} cluster which acts as a node (Fig. 1a), and then this node connects with four neighboring ones to form a 3-D diamond structure. The whole net has a 6-connected topology with a point symbol of $(3^6\cdot6^6\cdot7^3)$ (Fig. 1b). This 3-D inorganic framework shows alternate hexagonal channels along the *a* and *b* directions, which have windows of 9.215(4) × 5.470(3) $Å^2$ (Fig. 1c and S3†). The organic $(H_2DABCO)^{2+}$ cations were accommodated in the hexagonal channels through N–H···Cl hydrogen bonding interactions (Fig. 1d).

Compound **2** crystallizes in the monoclinic space group $P2(1)/c$, which is composed of another unprecedented 3-D $(Pb_{21}Cl_{59})^{17-}$ framework as well as organic $(Et_2DABCO)^{2+}$ dications and protonated water molecules (Fig. 2d). Different from the protonated DABCO dications in **1**, the DABCO molecule in **2** is ethylated during the synthesis. This *in situ N*-alkylation has been well developed in our group for synthesizing metal halide-based hybrids.[12] $(Et_2DABCO)^{2+}$ is larger than the $(H_2DABCO)^{2+}$ dication in size, which results in larger channels in the 3-D inorganic framework of **2**. There are eleven crystallographically independent Pb atoms in the structure and they are situated in a distorted octahedral or mono-capped prismatic coordination environment. Two different trigonal bipyramid shaped Pb_5Cl_{18} clusters are simplified to two kinds of nodes for the topological point of view (Fig. 2a). They have differences in the coordination environment of Pb, and connect with each other through three Cl bridging atoms (Cl16, Cl17, Cl18) in the *a* direction and two bridging Cl atoms (Cl11, Cl12) in the *b* direction (Fig. S4†). One node connects with three other neighboring nodes leading to an alveolate layer in the *bc* plane (Fig. 2b and c). These alveolate layers are further connected by the Pb6-centered octahedron to form a 3-D inorganic framework with 1-D channels in the *a* direction (Fig. S5†). This structure has a 4,5-connected net with a point symbol of $(3\cdot4^4\cdot5^2\cdot6^3)_4(3^2\cdot6^2\cdot7^2)$. The 3-D inorganic framework showed splayed channels with windows of 12.656(15) × 10.333(7) $Å^2$ (Fig. S5†). The $(Et_2DABCO)^{2+}$

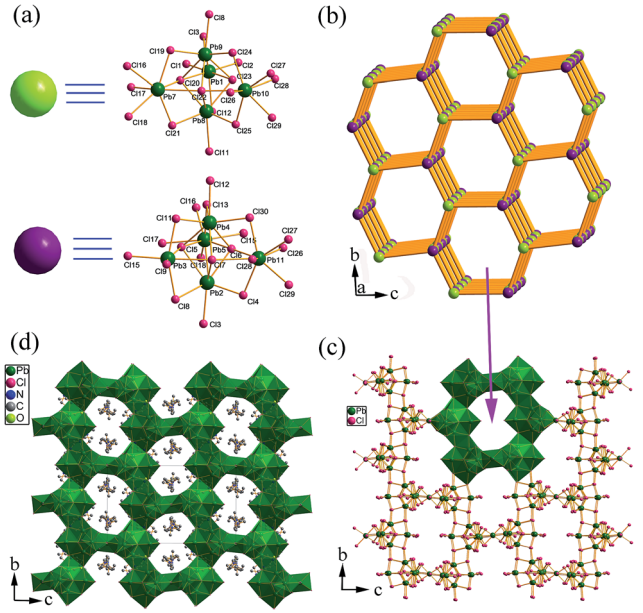

Fig. 2 For **2**: (a) topological nodes of the Pb_5Cl_{18} cluster; (b) topological structure of the $(Pb_{21}Cl_{59})^{2-}$ ions; (c) structure of the $(Pb_{21}Cl_{59}{}^{17-})$ framework viewed along the *a* axis, where parts of the Pb octahedra are shown as polyhedra; (d) crystal structure of compound **2** viewed along the *a* direction. Hydrogen atoms are omitted for clarity.

dications and protonated water molecules are located in the channels and contact with the 3-D $(Pb_{21}Cl_{59})^{17-}$ anions through Coulombic interactions (Fig. 2d).

Lead halide and its inorganic–organic hybrids normally are interesting p-type semiconductive materials. 3-D lead halide-based hybrid materials have shown impressive progress in solar cells with over 19% solar conversion efficiencies in recent years.[13] The electrical properties of **1** and **2** were determined using a two-probe direct current (DC) method with pressed pellets of the powdered samples from 30 to 170 °C. In an *I–V* curve, a steeper slope indicates a higher conductivity of a sample. As shown in Fig. S6a and S6c,† the conductivity of **1** is 2.18×10^{-7} S cm^{-1} at 30 °C, which gradually increases by raising the temperature and reaches 2.13×10^{-5} S cm^{-1} at 170 °C. The variety of the conductivity of **2** has a similar trend to that of **1**. It has a conductivity of 2.83×10^{-7} S cm^{-1} at 30 °C and 2.24×10^{-3} S cm^{-1} at 170 °C. Both the values and the trend of the conductivity increasing upon raising the temperature are very typical for semiconductive materials. The semiconductive properties of these hybrids should originate from the 3-D inorganic frameworks in the structures, which has been observed in other compounds in the same hybrid material family.[14] From optical absorption measurements (Fig. S7†), compound **2** has a smaller energy gap (E_g) than that of **1**. This might be an important reason why compound **2** has a more significant change in conductivity when varying the ambient temperature.

High CRI white-light emitting materials are very important for high-quality lighting. Here we show a possible way to create a high CRI single-component white-light emitting material using an organic and inorganic hybrid strategy. Compound **1** exhibits two emission peaks, centered at 455 (narrow peak, blue) and 585 nm (broad peak, yellow) (Fig. 3a). These two emissions should belong to different emitting centers due to the following two reasons. (1) They have a different maximum excitation (Fig. S8†): the blue one has a maximum excitation at 280 nm while the yellow one is at 320 nm. (2) They have different lifetimes (see Experimental section and Fig. S9 in the ESI†): 2.89 ns for 455 nm and 18.85 ns for 585 nm. Adjusting the excitation from 280 to 320 nm results in the intensity of the emission peak at 455 nm decreasing, while that at 585 nm increases. In this way, the emission of **1** can be modulated from blue to yellow. An intermediary excitation, 300 nm, is found to produce the "best" white-light emission with a quantum yield of 2.5%. The Commission Internationale de l'Eclairage (CIE) chromaticity coordinates of this white-light emission are (0.33, 0.34), which are very close to that of pure white light (0.33, 0.33) (Fig. 3c). The correlated color temperature (CCT) is 5393 K, corresponding to "cold" white light. Notably, the white-light emission of **1** shows a CRI value of 96. As far as we know, this value is the highest one reported for a single component white-light emitting compound, and well above the value for fluorescent light sources (~65) and reaches the value obtained by an expensive multi-component phosphor.

Similarly, compound **2** also has two emitting centers that are located at 420 (narrow peak, blue) and 690 nm (broad peak, orange) with lifetimes of 1.98 and 54.13 ns, respectively. It shows tunable photoluminescence from blue to orange upon variation of the excitation light (Fig. 3b and d). The maximum

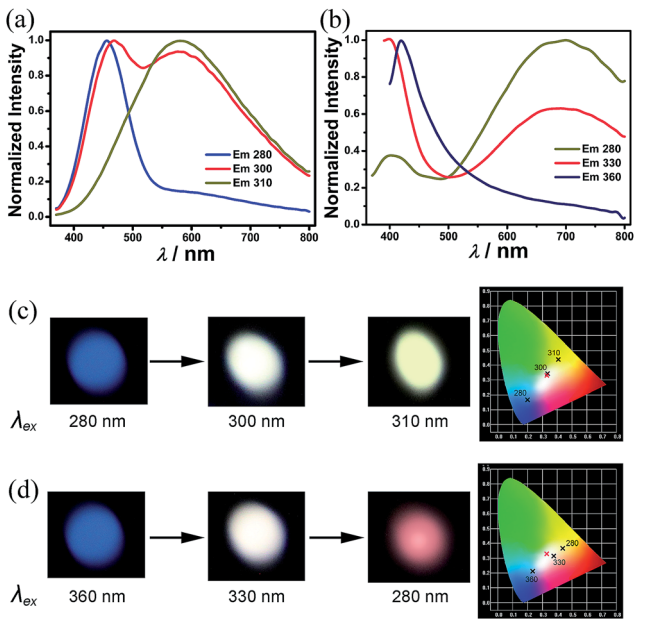

Fig. 3 Normalized solid-state photoluminescence spectra of **1** (a) and **2** (b) at room temperature upon variation of the excitation light; optical photographs of **1** (c) and **2** (d) excited by different wavelengths; CIE-1931 chromaticity diagram showing the emissions excited at 280, 300, and 310 nm for **1** (c), as well as 280, 330, and 360 nm for **2** (d), the red cross shows the position of pure white-light (0.33, 0.33).

excitation for the blue and orange emission is at 310 and 370 nm, respectively (Fig. S10†). Exciting compound **2** with light between the two maximum excitations can give a balanced ratio of blue and orange emission to produce white-light emission. The "best" excitation for white-light emission of **2** is 330 nm. At this excitation, the CIE chromaticity coordinates and quantum yield of the white-light emission are (0.38, 0.31) and 1%, respectively (Fig. 3d). Different from **1**, compound **2** shows a "warm" white light emission with a CCT value of 3496 K that is more preferable for indoor illumination. Its CRI is 88, less than that of **1**, but very close to the value for high-level applications.

Additionally, the PXRD and emission spectra of the two compounds are similar to their as synthesized ones, which indicate that these two compounds are stable at 280 °C (Fig. S11–S13†). **1** and **2** are also stable under photo-excitation; the intensity and peaks of the white light emission after constant irradiation for 48 h are close to those measured of their pristine samples (Fig. S14†).

It is well known that if the emission originates from the deep defects of a material, it will strongly depend on particle size and will be readily quenched by particle aggregation.[15] In **1** and **2**, similar emission spectra of larger than 10 μm-sized particles of hand-ground powder and 2–3 μm-sized particles of ball-milled powder were observed (Fig. S15–S18†). The emission centers are the same, only with a small difference in relative intensity. This indicates that the size of the sample has little influence on the emission, and the white-light emission of **1** and **2** is a bulk effect and not a result of surface defects.[9a]

The short lifetimes within the ns range for all of the emitting peaks of **1** and **2** indicate their fluorescence characteristics. To better understand the photoluminescence mechanisms, the emissions of $H_2(DABCO)Cl_2$, $[Et_2DABCO]I_2$ (see Experimental section and Fig. S19 and S20 in the ESI†) and bulk $PbCl_2$ were investigated. As shown in Fig. S21 and S22,† $H_2(DABCO)Cl_2$ displays a blue light emission centered at ~435 nm with a lifetime of 1.85 ns when excited at 370 nm; and $[Et_2DABCO]I_2$ also shows a blue light emission centered at 415 nm with a lifetime of 2.20 ns when excited at 345 nm. The positions and lifetimes of these emissions are comparable to the blue light emissions in **1** and **2**, demonstrating that the blue emissions in **1** and **2** originate from their organic components. Bulk $PbCl_2$ shows broad yellow light emission with a maximum peak at 545 nm and a lifetime of 4.70 ns (Fig. S22c and S23†), which is similar to the yellow/orange emission in **1** and **2**. These emissions can be assigned to a Pb-centered transition involving the s and p metal orbitals.[16] Owing to serious structural distortion between the ground and excited states, the emission of the s^2 compound shows a large shift from the absorption maxima, which has also been observed in **1** and **2**. The calculated energy between the s and p orbitals of Pb^{2+} in compound **2** is smaller than that of compound **1** (Fig. S24†), in accordance with the red shift emission of compound **2**. The inorganic 3-D structures in **1** and **2** play very important roles in showing such low energy emissions. $(Me_2DABCO)_2(PbCl_6)$ has a similar organic cation but a 0-D inorganic counterpart, which only shows blue emission from the organic part when varying the excitation (Fig. S25 and S26†). The mechanism of white-light emission in **1** and **2** is different from that of the recently reported 2-D layered hybrid perovskites (N-MEDA)$[PbBr_{4-x}Cl_x]$ and (EDBE)$[PbX_4]$.[9a,b] In these 2-D layered hybrid perovskites, the dielectric mismatch between the organic and inorganic layers results in multilayer quantum well structures and creates strongly bound excitons associated with the inorganic semiconducting layer. A broad distribution of intrinsic emissive trap states and strong electron–phonon coupling originating from the deformable lattice in the 2-D layered inorganic structure produce very broad emission for white light. So their white-light emission has only a contribution from the inorganic component, and the highest CRI in these compounds reported is 85. In our case, the white light emission is derived from the synergetic work of the inorganic and organic parts. The best advantage of our compounds is that the emission of the inorganic and organic components is relatively independent. The ratio of the emission from the inorganic and organic components could be flexibly tuned to enable us to produce white light with an ultra-high CRI.

Conclusions

In conclusion, two single-component white-light emitting hybrids have been reported in this work. One of them shows the highest CRI of 96 in single component phosphors to date. Their 3-D inorganic framework structures are unusual and play very important roles in the conducting properties and suitable long wavelength emission for white light. The blue emission of the organic component and yellow/orange emission of the inorganic component are independently tunable to produce a high CRI. Notably, compounds **1** and **2** also show multi-color emission, which may meet the requirements for colorful lighting or displays. In the future, lighting systems with low cost, long life, and high CRI are required to accurately mimic lighting conditions outside. Our work reports a new method to develop high performance white phosphors with systematically tunable emission properties.

Acknowledgements

This work was financially supported by the Financial support from the NSF of China (51402293, 21401193, 21471149, 21373225), and the NSF of Fujian Province (2014J01065, 2014J07003).

Notes and references

1 (*a*) K. Wooseok and J. Jing, *J. Am. Chem. Soc.*, 2008, **130**, 8114–8115; (*b*) D. F. Sava, L. E. S. Rohwer, M. A. Rodriguez and T. M. Nenoff, *J. Am. Chem. Soc.*, 2012, **134**, 3983–3986.

2 (*a*) L. Chen, K.-J. Chen, S.-F. Hu and R.-S. Liu, *J. Mater. Chem.*, 2011, **21**, 3677–3685; (*b*) A. A. Setlur, W. J. Heward, Y. Gao, A. M. Srivastava, R. G. Chandran and M. V. Shankar, *Chem. Mater.*, 2006, **18**, 3314–3322; (*c*) Y. Li, A. Rizzo, R. Cingolani and G. Gigli, *Adv. Mater.*, 2006, **18**, 2545–2548; (*d*) X.-H. Zhu, J. Peng, Y. Cao and J. Roncali, *Chem. Soc. Rev.*, 2011, **40**, 3509–3524; (*e*) N. Guo, H. You, Y. Song, M. Yang,

K. Liu, Y. Zheng, Y. Huang and H. Zhang, *J. Mater. Chem.*, 2010, **20**, 9061–9067.

3 (*a*) M. Roushan, X. Zhang and J. Li, *Angew. Chem., Int. Ed.*, 2012, **51**, 436–439; (*b*) C.-C. Shen and W.-L. Tseng, *Inorg. Chem.*, 2009, **48**, 8689–8694; (*c*) S. Sapra, S. Mayilo, T. A. Klar, A. L. Bogach and J. Feldmann, *Adv. Mater.*, 2007, **19**, 569–572.

4 (*a*) S. Ye, F. Xiao, Y. X. Pan, Y. Y. Ma and Q. Y. Zhang, *Mater. Sci. Eng., R*, 2010, **71**, 1–34; (*b*) J. Silver, R. Withnall and A. Kitai, *Luminescent Materials and Applications*, John Wiley & Sons, Chicester, 2008, p. 75.

5 (*a*) M.-S. Wang, S.-P. Guo, Y. Li, L.-Z. Cai, J.-P. Zou, G. Xu, W.-W. Zhou, F.-K. Zheng and G.-C. Guo, *J. Am. Chem. Soc.*, 2009, **131**, 13572–13573; (*b*) G.-P. Yong, Y.-M. Zhang, W.-L. She and Y.-Z. Li, *J. Mater. Chem.*, 2011, **21**, 18520–18522; (*c*) Y. Liu, M. Pan, Q.-Y. Yang, L. Fu, K. Li, S.-C. Wei and C.-Y. Su, *Chem. Mater.*, 2012, **24**, 1954–1960; (*d*) K. T. Kamtekar, A. P. Monkman and M. R. Bryce, *Adv. Mater.*, 2010, **22**, 572–582; (*e*) M. C. Gather, A. Köhnen and K. Meerholz, *Adv. Mater.*, 2011, **23**, 233–248; (*f*) Z.-F. Liu, M.-F. Wu, S.-H. Wang, F.-K. Zheng, G.-E. Wang, J. Chen, Y. Xiao, A.-Q. Wu, G.-C. Guo and J.-S. Huang, *J. Mater. Chem. C*, 2013, **1**, 4634–4639; (*g*) X. Fang, M. Roushan, R. Zhang, J. Peng and H. Zeng, *Chem. Mater.*, 2012, **24**, 1710–1717; (*h*) H.-B. Xu, X.-M. Chen, Q.-S. Zhang, L.-Y. Zhang and Z.-N. Chen, *Chem. Commun.*, 2009, 7318–7320; (*i*) S. Dang, J.-H. Zhang and Z.-M. Sun, *J. Mater. Chem.*, 2012, **22**, 8868–8873; (*j*) M. Shang, C. Li and J. Lin, *Chem. Soc. Rev.*, 2014, **43**, 1372–1386.

6 (*a*) X.-H. Zhu, J. Peng, Y. Cao and J. Roncali, *Chem. Soc. Rev.*, 2011, **40**, 3509–3524; (*b*) R. M. Adhikari, L. Duan, L. Hou, Y. Qiu, D. C. Neckers and B. K. Shah, *Chem. Mater.*, 2009, **21**, 4638–4644; (*c*) Y. Liu, M. Nishiura, Y. Wang and Z. Hou, *J. Am. Chem. Soc.*, 2006, **128**, 5592–5593.

7 Y. J. Tung, M. M. H. Lu, M. S. Weaver, M. Hack and J. J. Brown, *Proc. SPIE*, 2004, **5214**, 114–123.

8 M. S. Park, H. J. Park, O. Y. Kim and J. Y. Lee, *Org. Electron.*, 2013, **14**, 1504–1509.

9 (*a*) E. R. Dohner, A. Jaffe, L. R. Bradshaw and H. I. Karunadasa, *J. Am. Chem. Soc.*, 2014, **136**, 13154–13157; (*b*) E. R. Dohner, E. T. Hoke and H. I. Karunadasa, *J. Am. Chem. Soc.*, 2014, **136**, 1718–1721; (*c*) C.-Y. Sun, X.-L. Wang, X. Zhang, C. Qin, P. Li, Z.-M. Su, D.-X. Zhu, G.-G. Shan, K.-Z. Shao, H. Wu and J. Li, *Nat. Commun.*, 2013, **4**, 1–8.

10 (*a*) D. B. Mitzi, S. Wang, C. A. Feild, C. A. Chess and A. M. Guloy, *Science*, 1995, **267**, 1473–1476; (*b*) D. B. Mitzi, K. Chondroudis and C. R. Kagan, *IBM J. Res. Dev.*, 2001, **45**, 29–45; (*c*) N. Leblanc, W. Bi, N. Mercier, P. Auban-Senzier and C. Pasquier, *Inorg. Chem.*, 2010, **49**, 5824–5833.

11 (*a*) Z.-J. Zhang, S.-C. Xiang, G.-C. Guo, G. Xu, M.-S. Wang, J.-P. Zhou, S.-P. Guo and H.-S. Huang, *Angew. Chem., Int. Ed.*, 2008, **47**, 4149–4152; (*b*) D. B. Mitzi, *Prog. Inorg. Chem.*, 1999, **48**, 1–121; (*c*) J. D. Martin and K. B. Greenwood, *Angew. Chem., Int. Ed.*, 1997, **36**, 2072–2075.

12 (*a*) G.-E. Wang, X.-M. Jiang, M.-J. Zhang, H.-F. Chen, B.-W. Liu, M.-S. Wang and G.-C. Guo, *CrystEngComm*, 2013, **15**, 10399–10404; (*b*) G.-E. Wang, M.-S. Wang, X.-M. Jiang, Z.-F. Liu, R.-G. Lin, L.-Z. Cai, G.-C. Guo and J.-S. Huang, *Inorg. Chem. Commun.*, 2011, **14**, 1957–1961; (*c*) G. Xu, G.-C. Guo, J.-S. Huang, S.-P. Guo, X.-M. Jiang, C. Yang, M.-S. Wang and Z.-J. Zhang, *Dalton Trans.*, 2010, 8688–8692; (*d*) G. Xu, G.-C. Guo, M.-S. Wang, Z.-J. Zhang, W.-T. Chen and J.-S. Huang, *Angew. Chem., Int. Ed.*, 2007, **46**, 3249–3251; (*e*) G. Xu, Y. Li, W.-W. Zhou, G.-J. Wang, X.-F. Long, L.-Z. Cai, M.-S. Wang, G.-C. Guo, J.-S. Huang, G. Bator and R. Jakubas, *J. Mater. Chem.*, 2009, **19**, 2179–2183.

13 (*a*) M. Z. Liu, M. B. Johnston and H. J. Snaith, *Nature*, 2013, **501**, 395–398; (*b*) J. Burschka, N. Pellet, S.-J. Moon, R. Humphry-Baker, P. Gao, M. K. Nazeeruddin and M. Gratzel, *Nature*, 2013, **499**, 316–319; (*c*) H. Zhou, Q. Chen, G. Li, S. Luo, T. Song, H.-S. Duan, Z. Hong, J. You, Y. Liu and Y. Yang, *Science*, 2014, **345**, 542–546; (*d*) N. J. Jeon, J. H. Noh, Y. C. Kim, W. S. Yang, S. Ryu and S. Seok II, *Nat. Mater.*, 2014, **13**, 897–903.

14 (*a*) A. Jaffe, Y. Lin, W. L. Mao and H. I. Karunadasa, *J. Am. Chem. Soc.*, 2015, **137**, 1673–1678; (*b*) Z. Xu, D. B. Mitzi, C. D. Dimitrakopoulos and K. R. Maxcy, *Inorg. Chem.*, 2003, **42**, 2031–2039; (*c*) C. C. Stoumpos, C. D. Malliakas and M. G. Kanatzidis, *Inorg. Chem.*, 2013, **52**, 9019–9038.

15 M. J. Bowers, J. R. McBride and S. J. Rosenthal, *J. Am. Chem. Soc.*, 2005, **127**, 15378–15379.

16 R. Kink, T. Avarmaa, V. Kisand, A. Lõhmus, I. Kink and I. Martinson, *J. Phys.: Condens. Matter*, 1998, **10**, 693–700.